Mon. Not. R. Astron. Soc. **283,** 551–565 (1996)

The flux of meteorites to the Earth over the last 50 000 years

P. A. Bland,[1] T. B. Smith,[2] A. J. T. Jull,[3] F. J. Berry,[4] A. W. R. Bevan,[5] S. Cloudt[3] and C. T. Pillinger[1]

[1]*Planetary Science Research Institute, The Open University, Walton Hall, Milton Keynes MK7 6AA*
[2]*Department of Physics, The Open University, Walton Hall, Milton Keynes MK7 6AA*
[3]*NSF Accelerator Facility for Radioisotope Analyses, University of Arizona, Tucson, Arizona 85721, USA*
[4]*Department of Chemistry, The Open University, Walton Hall, Milton Keynes MK7 6AA*
[5]*Department of Earth and Planetary Sciences, Western Australian Museum, Perth, Western Australia, 6000*

Accepted 1996 July 3. Received 1996 July 1; in original form 1996 March 15

ABSTRACT

98 ordinary chondrite finds, terrestrial age-dated using ^{14}C analyses by Jull et al., from three arid/semi-arid meteorite accumulation sites (New Mexico, the Sahara, and the Nullarbor Region, Australia) have been examined by Mössbauer spectroscopy to determine quantitatively the terrestrial oxidation for each sample. A comparison of weathering over time, and its effect in 'eroding' meteorites, allows a calculation of a decay constant for meteorites from each hot desert site. This, together with the number and mass distribution of paired meteorites in each region, enables us to derive estimates of the number of meteorite falls over a given mass per year: we calculate between 36 and 116 falls over 10 g per 10^6 km^2 yr^{-1}. In addition, we constrain the total mass flux to the Earth's surface over the 10 g to 1 kg interval to between 2900 and 7300 kg yr^{-1}. We find remarkable agreement in our estimates from each accumulation site, and also with the estimate of the present flux made from MORP camera network data presented by Halliday, Blackwell & Griffin, suggesting that the flux of meteorites to the Earth has remained essentially constant over the last 50 000 yr. This work is the first independent confirmation of the MORP estimate, and indicates that meteorite accumulation sites provide an alternative method of calculating flux. We suggest that the application of a similar methodology to the Antarctic meteorite population may be used to explore the possibility that the flux of meteorites to the Earth has varied over the 1-Ma time-scale sampled by these meteorites.

Key words: meteors, meteoroids.

1 INTRODUCTION

An accurate determination of the flux of meteorites to the Earth's surface has importance in constraining models of the cratering history of the inner Solar system and the orbital evolution of asteroids and comets, and in quantifying the frequency of large impacts to the Earth. In this paper we adopt a novel approach to the problem of estimating flux, based on an analysis of the oxidation and loss by weathering of ordinary chondrites which have accumulated in hot deserts over approximately the last 50 000 yr.

A number of previous attempts have been made to quantify the accretion rate of the total mass of extraterrestrial material, or the portions of it represented by cosmic dust, meteorites or large asteroid/comet impacts. Estimates of the total flux of extraterrestrial particles have generally relied on the use of geochemical methods to determine the concentration of a diagnostic component in sediments, e.g., Ir (Barker & Anders 1968; Ganapathy 1983; Kyte & Wasson 1986), Os (Esser & Turekian 1988), cosmogenic ^{53}Mn (Bibron et al. 1974; Imamura et al. 1979) and ^{3}He (Ozima et al. 1984; Takayanagi & Ozima 1987; Farley 1995; Farley & Patterson 1995), and magnetic spherules in deep-sea sediments or ice caps (Murrell, Davis & Nishiizumi 1980; Maurette et al. 1987). An important point to consider with these estimates is that, given the sedimentary time-scales involved, it is unlikely that material resulting from the larger crater-forming events will be sampled. As such, current esti-

mates of the total flux of extraterrestial particles must be considered minimum values. Although this work has furnished a reasonably consistent total mass flux [on the order of $(5–10) \times 10^7$ kg yr^{-1}] averaged over the last few tens of thousands of years, it tells us little about the mass distribution of the flux, i.e., the number per year of falls within a given mass range.

Various studies have adopted very different approaches to estimate flux in different areas of the mass distribution. Fig. 1 shows a comparison of these estimates. A direct measurement of the mass accretion rate of cosmic dust (in the mass range 10^{-9} to 10^{-4} g) was made using the *Long Duration Exposure Facility* satellite (Love & Brownlee 1993), which yielded an estimate of $(40 \pm 20) \times 10^6$ kg yr^{-1}. A recalculation of the mass–velocity relation, based on new data of atmospheric encounter speeds (Taylor 1995), suggests that the mass distribution and cumulative flux curve for the above size range estimated by Love & Brownlee (1993) is actually very close to that of Grün et al. (1985). These and other estimates of flux for cosmic dust yield a reasonably consistent estimate of $(30–40) \times 10^6$ kg yr^{-1}.

Estimates of the asteroid and comet flux to the Earth, and the cratering rate (i.e., the flux of the largest mass fraction) have been made by interpreting the cratering history of the Moon, Mercury and Mars (Barlow 1990), and also in the (far from complete) geological record of the Earth (Grieve 1984). Extrapolations from the small population of observed Earth-crossing asteroids have resulted in estimates of the probability of collision of these objects with the Earth (Shoemaker et al. 1990; Rabinowitz 1993). Given the assumptions involved, the results are reasonably consistent: Barlow (1990) calculates approximately 6.5×10^{-7} events per year producing craters in excess of 32-km diameter (equivalent to an impactor of mass 3.1×10^{13} kg for an astroid of density 2.2 g cm^{-3}), which is similar to the estimate of Grieve (1984) and Shoemaker, Wolfe & Shoemaker (1990). The estimate of Rabinowitz (1993) is slightly higher, perhaps due to the (probably) unrealistically high asteroid density of 3.5 g cm^{-3} used in this study.

Although attempts to determine the frequency of micrometeorite and crater-forming events have yielded consistent estimates of flux for these portions of the mass distribution, the same is not true for the (intermediate) meteorite size range.

Initial attempts to determine the flux of meteorites in the mass range 10 to 10^6 g (i.e., typical fireballs and meteorite falls) used data on the recovery of eye-witnessed falls in densely populated areas (Brown 1960, 1961; Hawkins 1960; Millard 1963; Buchwald 1975; Hughes 1980). Unfortunately, estimates of flux calculated using this technique have varied by more than 4 orders of magnitude, probably as a result of the difficulty of unambiguously constraining a number of parameters inherent in this method, e.g., population density, season, time of day, etc. More recently, direct observations of fireball events using camera networks have provided an estimate of the present flux of meteorites and

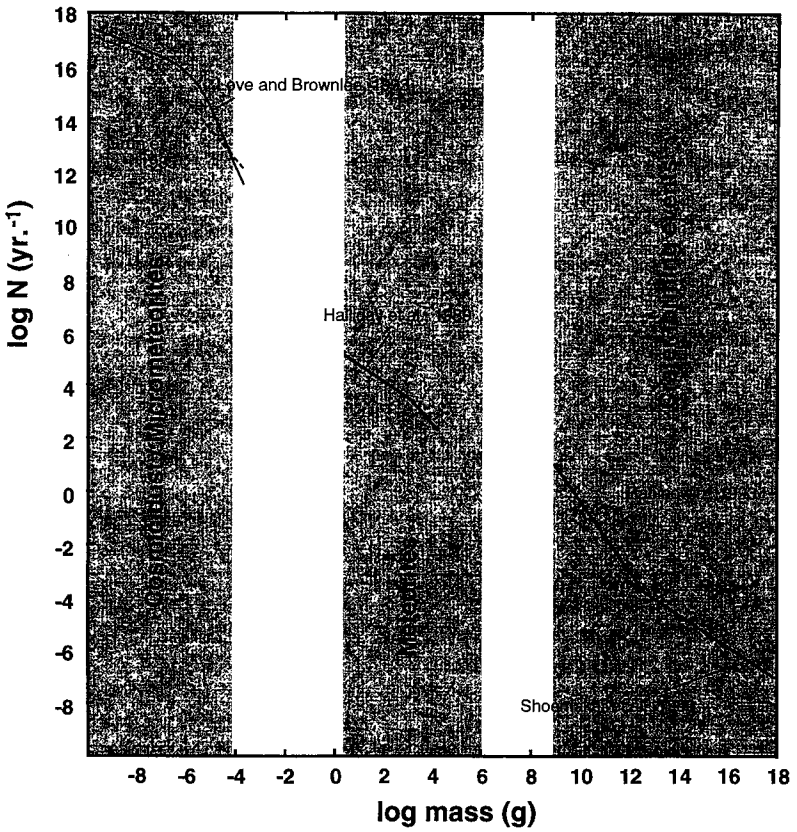

Figure 1. Number of bodies accreted to the surface of the Earth ($\log N$ yr^{-1}), for a large portion of the mass distribution of extraterrestrial material, as a function of mass (in g) as determined by previous authors.

its mass distribution. In particular, data from the MORP camera network (Halliday, Blackwell & Griffin 1989) suggest a present flux of 8.7 events of mass equal to or greater than 1 kg per 10^6 km^2 per year. To our mind, this is the single best estimate of meteorite flux to date. Given that only one well-constrained data set exists, and considering that flux in the meteorite size range constrains values for high-mass micrometeorites and low-mass crater-forming events (see Fig. 1), an independent experimental critique of the MORP results would be valuable.

Another method for calculating flux, and possibly also temporal variations in flux, involves analyses of meteorite accumulation sites. The method was outlined by Huss (1990) and Zolensky, Wells & Rendell (1990). The idea behind this approach is that if the number of meteorite samples per unit area on the ground today is known, and the rate at wich they are removed by weathering (characterized by a so-called 'decay constant') is calculated, then we can work back to derive an estimate of the number that fell to Earth initially. This paper addresses this method, its possibilities and its pitfalls.

Sections 2 and 3 include a discussion of the methodology of this approach, how previous studies may have failed to address adequately some of the associated problems, and our own experimental procedure. In Section 4, we begin by calculating a decay constant based solely on terrestrial age data for all our hot desert meteorite samples (98 in number), and show how a decay constant may also be obtained by considering both oxidation and terrestrial age data together. However, such a global approach may be an oversimplification. In Section 4.2 we also investigate the effect of bulk initial chemistry on weathering rate, i.e. whether different decay constants exist for high-iron (H group) or low-iron [L(LL) group] ordinary chondrites. In Section 4.3 we discuss how differences in weathering rate may arise essentially from 'environmental' factors, i.e., variations due to climate and geomorphology between accumulation sites. In Section 5 we discuss the acquisition of mass distribution and population density data (i.e., number of meteorites per unit area) for samples from three hot desert accumulation sites and, by combining these data with estimates of the decay constant, derive three independent estimates of the flux of meteorites to the Earth (Section 6). The paper concludes with a discussion of the significance of these findings and how our estimates of flux compare to those in the literature.

2 ESTIMATING METEORITE FLUX FROM ACCUMULATION SITES

There are several locations on Earth where, under favourable conditions, meteorites may accumulate. Amongst these are numerous hot desert sites, including the Sahara Desert (SD), Roosevelt County, New Mexico (RC) and the Nullarbor Region (NR) of Australia, and also the cold desert of Antarctica. In theory, these accumulation sites should record the integrated flux throughout the meteorite mass range over the lifetime of the accumulation surface. Thus, given knowledge of meteorite weathering rates (usually gained through plotting frequencies of meteorite terrestrial ages), it should be possible to discern changes in flux and mass distribution with time (hot deserts retain meteorites for up to 50 000 yr, whilst meteorites may survive in Antactica for over 10^6 yr). However, there are several problems with this approach.

(1) An accurate age for either the accumulation surface and/or terrestrial ages for the meteorite population is required.
(2) The action of weathering in removing samples must be quantified.
(3) Other processes may act to remove samples.
(4) All the meteorite samples within a given area must be recovered, and a study to 'pair' samples undertaken: meteorites commonly fragment on entering the Earth's atmosphere, so that one meteorite might be represented by a large number of stones.
(5) In any one meteorite fall, samples may be scattered over a large area – a strewn field. If the search area is small compared to the typical strewn field, then it may sample more falls than are representative of the area itself.

Owing to one or more of the above factors, previous attempts to calculate meteorite flux based on data from accumulation sites have differed by approximately an order of magnitude (Huss 1990; Zolensky et al. 1990) from data for a similar mass range derived from camera studies (Halliday et al. 1989). A major problem lies in deriving a meaningful decay constant for a meteorite population: poorly constrained age data for accumulation surfaces, and sparse or poorly constrained terrestrial ages for meteorites, lead to large errors when calculating a value for the decay constant. Huss (1990) used one age determination for the surface of the meteorite accumulation site at RC which was subsequently found to be unrepresentative of the area as a whole (Zolensky et al. 1992). In a similar study, Zolensky et al. (1990) calculated a value for the decay constant for the same area using a cumulative frequency curve of only eight meteorite terrestrial ages, none of which was actually recovered from RC itself.

Whilst these earlier studies succeeded in defining a method by which meteorite accumulation sites might provide an estimate of flux, there is clear potential for improvement, and an obvious requirement for verification of the present estimate of the flux of meteorites to the Earth. Meteorite accumulation sites provide a valuable opportunity to assess meteorite flux, and to discern possible temporal flux variations over the lifetime of the accumulation sites.

3 EXPERIMENTAL ANALYSIS

This study looks in detail at weathering in samples of 98 ordinary chondrites, from three hot desert regions, for which terrestrial age data are available. Throughout this work our discussion considers paired meteorite samples, thus quoted masses and population density estimates are for surviving meteorites, not fragments. By comparing the terrestrial age of the sample with an independent, quantitative measure of weathering (the percentage of total iron as ferric iron derived from Mössbauer spectra), we arrive at alternative estimates of the decay constant to those obtained by using terrestrial age data alone. The approach is a development of that outlined in Bland et al. (1996a), and employs a much larger data set to derive flux estimates for three sites,

whilst the earlier paper considered only RC. Our analysis is principally concerned with the rate at which meteorites are removed by weathering; it is therefore necessary to consider which intrinsic properties and extrinsic processes are important in controlling meteorite weathering rates.

3.1 Meteorites

80–90 per cent of meteorites are ordinary chondrites whose classification scheme is based on the abundance of reduced iron (Fe^0) and Fe^{2+}-containing minerals [both high iron (H) and low iron (L and LL) groups exist]. In a hot desert environment, these iron-bearing minerals begin a gradual change to clay mineraloids and iron oxides/oxyhydroxides (principally of Fe^{3+} valence state) through weathering. To monitor weathering over time, we have acquired Mössbauer spectra from ordinary chondrites from three hot desert sites: the SD, the RC and the NR. Mössbauer spectroscopy allows the nature and relative abundance of Fe-containing phases in a sample to be determined; as such, it may be used to determine the degree of terrestrial oxidation experienced by a meteorite (Bland, Berry & Pillinger 1995). All the specimens are of known terrestrial age, determined by ^{14}C measurement (Jull et al. 1990, 1991, 1993a, 1995), and pairing studies have been undertaken (see Section 5). The hot desert meteorites discussed in this work constitute all of those for which terrestrial age data are currently available.

3.2 Mössbauer spectroscopy

^{57}Fe Mössbauer spectra were recorded from samples (0.3 g) at 298 K with a microprocessor-controlled Mössbauer spectrometer using a $^{57}Co/Rh$ source. Individual spectra took approximately 3 d to record. The drive velocity was calibrated with the same source and a metallic iron foil. Mössbauer spectra were fitted with a constrained non-linear least-squares fitting program of Lorentzian functions. The fitted lines were integrated to give the relative area intensities of the iron-containing phases in the sample. Generally, 3–4 distinct Fe^{3+}-bearing components were recognized. In this study the spectral areas of these components have been combined to give an overall percentage oxidation for a meteorite sample. In an independent study to establish the error in determining oxidation from Mössbauer spectroscopy of meteorites, Bland et al. (1996b) observed a 1.4 per cent relative error in the spectral area of ferric components in repeat analyses of the same meteorite aliquot (essentially an analytical error). In a similar study, Benoit et al. (1996) observed a 5 per cent relative error for spectra recorded from different paired stones of the same meteorite fall. This second, larger, error also includes the 'geological' uncertainty in comparing the weathering of widely scattered fragments of the same original meteorite fall, and is more meaningful in the context of this present work (e.g., Fig. 2).

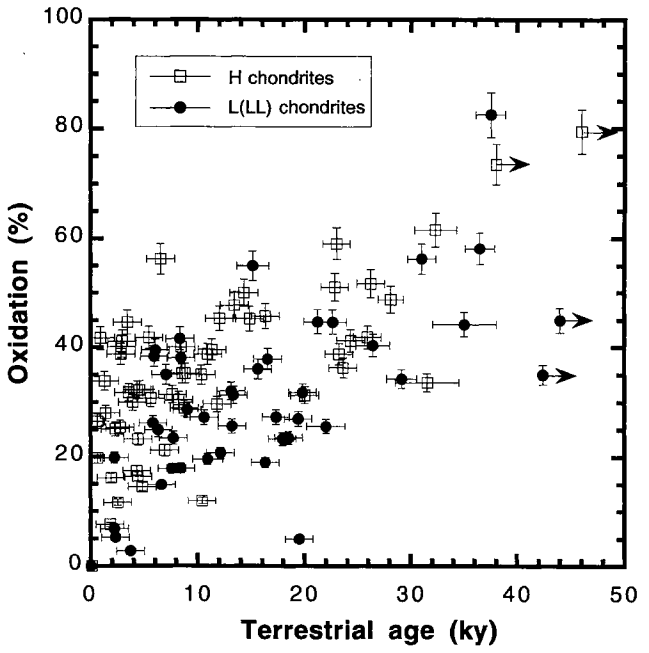

Figure 2. Scatter plot for 98 H and L(LL) chondrites, showing terrestrial age and oxidation percentage for each sample.

4 ESTIMATES OF THE DECAY CONSTANT

Initially, in Section 4.1, we shall combine oxidation and age data for both H and L(LL) chondrites from all three locations as a single data set, and use that to calculate an average decay constant for chondrites falling in arid/semi-arid regions. In Section 4.2, we consider H and L(LL) meteorites separately. Finally, in Section 4.3, we consider each site independently, and argue that there are factors unique to each area which make a 'global' analysis an oversimplification.

4.1 All hot desert sites

To describe our theoretical method we begin by considering all 98 meteorites together. Percentage oxidation, obtained using Mössbauer spectroscopy, and published terrestrial age data (Jull et al. 1990, 1991, 1993a, 1995) are plotted for each sample [separated for H and L(LL) group chondrites] in Fig. 2. We shall base our analysis on the customary 'radioactive decay' model (Zolensky et al. 1990; Jull et al. 1993b). According to this model, if $n_0(m)\,dt$ meteorites of incoming mass exceeding m fall per unit area during interval dt, then, for steady state, the number surviving to age t will be $n(t)\,dt$, where flux n_0 is time-independent and

$$n(t) = n_0(m)\exp(-\lambda t). \tag{1}$$

Then, if one selects a defined area A and identifies the number of surviving meteorites, n_{tot}, for that area, we must have

$$n_{tot} = A\int_0^\infty n(t)\,dt = A\,n_0(m)/\lambda,$$

so that the flux estimate would be

$$n_0(m) = \lambda\left(\frac{n_{tot}}{A}\right). \tag{2}$$

We take this to be the definition of the decay constant λ. Clearly, A should be larger, rather than smaller, to minimize

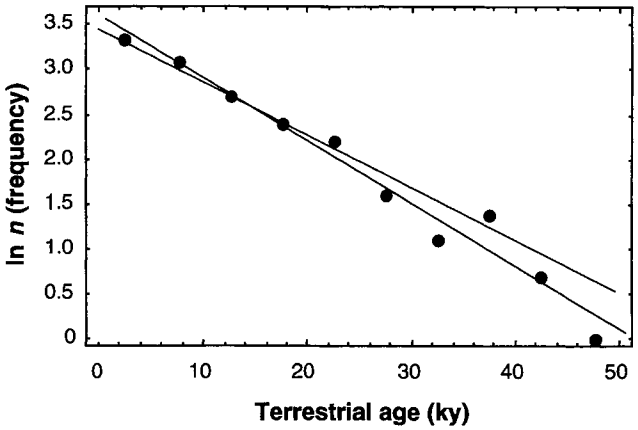

Figure 3. The data of Fig. 2 arranged to show the natural logarithm (ln) of the number n versus age in kyr, with bins of 5 kyr. The lines have slopes -0.59 and -0.70.

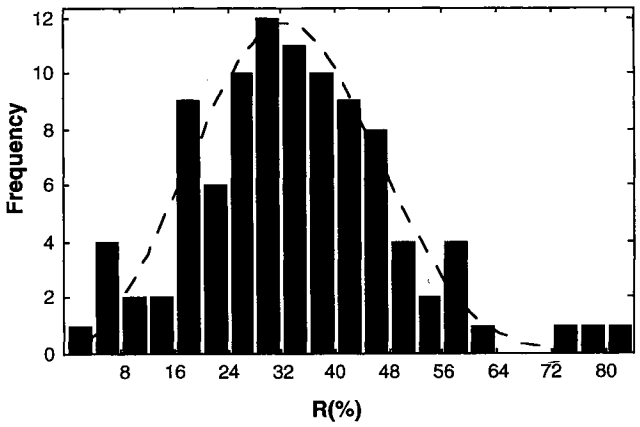

Figure 4. The data of Fig. 2 arranged to show number versus oxidation (per cent) with bins of width 4 per cent, and a comparison with the theory from equation (8).

statistical fluctuations (Halliday, Blackwell & Griffin 1991). Up to now, only the relatively small area of 11 km^2 in RC (Zolensky et al. 1990) has been combed for all specimens. In this work we also present similar data for the NR and the SD, based on areas of these regions that have been systematically searched.

Equation (2) emphasizes that an estimate for the flux $n_0(m)$ requires two things: for a given region of area A one needs, first, a value for the decay constant λ and, secondly, an estimate of $n_{\rm tot}$, the total number of paired meteorites on the ground from falls of mass greater than m. In this section we concentrate on estimating λ.

Since terrestrial ages have been obtained for each meteorite, a relatively direct estimate of the decay constant λ follows from the relationship between the relative number of samples and sample age. A similar method was employed by Zolensky et al. (1990) and applied to the RC population, using a cumulative frequency distribution based on only eight samples. In Fig. 3 we have scaled the data to kiloyears, distributed the data (98 samples) into bins of width of 5 kyr, and plotted $\ln(n)$ versus t so that the slope gives an estimate of $-\lambda$. The two lines in Fig. 3 represent roughly extreme cases, and have slopes of -0.059 and -0.070, so that, apart from any possible systematic errors, this method implies $\lambda = 0.065 \pm 0.005$ kyr^{-1}. Whilst the terrestrial age data set is statistically fairly large for all hot deserts lumped together, a similar analysis for individual sites is less reliable: for geomorphologic and climatic reasons, meteorites with old or very young terrestrial ages may be absent from a population, leading to a distortion of an ideal frequency distribution. In addition, data sets for individual sites are typically small. However, our method separately relates the degree of oxidation (on average) to time on Earth, and thereby gains a further insight into the weathering process. By considering two independent variables, the model is more resilient, given problems of incomplete or small data sets. Initially, however, we shall continue to consider all 98 samples together to expound the method.

The histogram of Fig. 4 shows the distribution of all 98 meteorites with respect to the degree of oxidation (R per cent). The general shape of this distribution is consistent with an initial rapid period of oxidation, until at around 30–50 per cent oxidation the available porosity in the sample is filled. Unweathered ordinary chondrite falls are quite porous, similar to a terrestrial sandstone, so it is likely that up to a certain point the production of ferric phases, and concomitant volume expansion, does not lead to meteorite fragmentation. However, once this critical point is reached, continued oxidation leads to destructive fragmentation and the eventual total loss of the sample by erosion.

To combine the two features of oxidation and erosion, we seek a relationship between R and t, and use equation (1) to represent the average loss by erosion. To model $R(t)$, we split the data of Fig. 2 into time bins of varying width so as to ensure that about four data points fell in each bin. For each bin the mean, $R_{\rm av}$, was calculated, scaled to the interval $(0, 1)$, and $\ln(R_{\rm av})$ was plotted versus $\ln t$ (Fig. 5). Also shown in Fig. 5 are fits to the data of the form

$$\ln R = \ln a + b \ln t, \tag{3}$$

which correspond to the choices $(-1.75, 0.33)$ and $(-1.90, 0.33)$ for $(\ln a, b)$. The suggestion here then is a power law of the form

$$R(t) = at^b \tag{4}$$

to describe the (smoothed) relationship between time and oxidation. The function $R(t)$ has a form which is consistent with the idea that initial oxidation should be very fast (in fact, this expression has infinite slope $\dot{R}$ at $t = 0$), but as time increases, will slow down. The fact that $R(t)$ will exceed unity for high values of t has no important repercussions, since by that time essentially no specimens remain.

To model the shape of the oxidation–frequency histogram (Fig. 4), we combine sample loss with ferric alteration by noting that the number with age between t and $t + {\rm d}t$ is the same as the number with oxidation between R and $R + {\rm d}R$, namely $n(t)\,{\rm d}t = N(R)\,{\rm d}R$, so $N(R) = n(t)\,{\rm d}t/{\rm d}R$. To get $N(R)$, we find $t(R)$ from equation (4), namely $t = R^{1/b} a^{-1/b}$. Then, from equation (1),

$$n = n_0\, {\rm e}^{-\lambda R^{1/b} a^{-1/b}}.$$

Differentiating $t(R)$ gives

$$\frac{dt}{dR}=\frac{1}{a^{1/b}}\frac{1}{b}R^{1/b-1},$$

and so

$$N(R)=n_0\,e^{-\lambda(R/a)^{1/b}}\left(\frac{1}{ba^{1/b}}\right)R^{(1-b)/b}=KR^{(1-b)/b}\,e^{-\lambda(R/a)^{1/b}},$$

where K is a constant.

In our case, b lies between zero and unity. Then $N(R)$ vanishes at $R=0$ and, for small R, increases like $R^{(1-b)/b}$. At larger R, the exponential factor dominates and forces $N(R)$ to decrease from a single maximum. If this maximum occurs at $R=R^*$, then dN/dR vanishes there. Equating to zero the first derivative of $N(R)$ and solving for R gives

$$R^*=a\left(\frac{1-b}{\lambda}\right)^b. \tag{5}$$

Thus, for instance, knowledge of a, b and R^* would give λ as

$$\lambda=(1-b)\left(\frac{a}{R^*}\right)^{1/b}. \tag{6}$$

Note that since equation (4) relates R and t, we can define a time t^* by $R^*=a(t^*)^b$ and rewrite the decay constant as

$$\lambda=\frac{(1-b)}{t^*}. \tag{7}$$

Finally, if the maximum of N is defined as $N^*\equiv N(R^*)$, one can write

$$N(R)=N^*\exp(1-b)\left(\frac{R}{R^*}\right)^{(1-b)/b}\exp\left[-(1-b)\left(\frac{R}{R^*}\right)^{1/b}\right]. \tag{8}$$

Equation (8) gives the prediction of our simple model, with density $N(R)$ depending upon three parameters: N^*, R^* and b. One further parameter is a, which occurs in expression (4) for $R(t)$. The particular importance of a is that it enters into our estimate for λ, equation (6). Fig. 4 shows expression (8) for $N(R)$ superposed on the data, where we have varied R^*, N^* and b to give a good fit-by-eye under the further condition that the areas under $N(R)$ and the histogram be equal. For the data shown we found $R^*=0.346$, $N^*=11.77$ and $b=0.33$. Further, using the fits to $R(t)$ in Fig. 5 gives $a=\exp(-1.75)=0.17$ and $a=\exp(-1.90)=0.15$. Using these values in equation (6) gives corresponding estimates of 0.078 and 0.053 kyr^{-1} for λ, and values of 8.6 and 12.6 kyr for t^* (from equation 7). Thus our two estimates for λ, one directly from the time decay and the other from analysis of ferric alteration data, are in good agreement.

We note parenthetically that (following through the algebra) the maximum $N^*=N(R^*)$ can be expressed as

$$N^*=\frac{n_0}{ab}(t^*)^{1-b}\,e^{-\lambda t^*}. \tag{9}$$

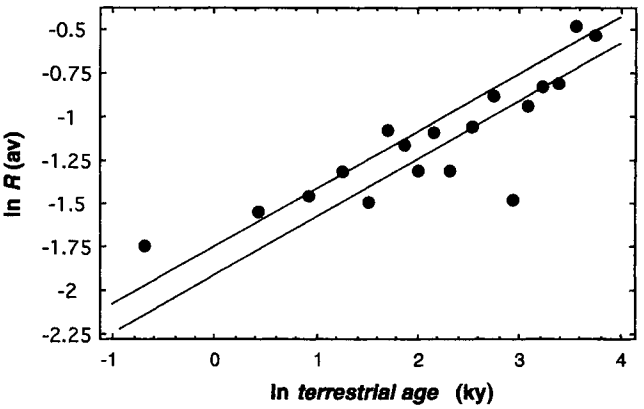

Figure 5. The data of Fig. 2 binned to varying values of t, scaled to the interval (0, 1), and ln of the (average) oxidation plotted versus ln of the age (kyr). The lines have slope 0.33.

Thus, if it were possible to scour a (large) specified area for *all* distinct surviving meteorites of mass greater than m, then an application of this method as we have described it would give values for N^*, a and b, and hence also λ and t^*, resulting in a direct estimate of $n_0(m)$ via equation (9).

4.2 H and L(LL) chondrites separated

The data presented in Fig. 2 suggest that H and L(LL) chondrites show a systematic difference in the rate at which they are oxidized. Figs 6(a) and (b) show plots of $\ln(n)$ versus t separately for H (55 samples) and L(LL) chondrites (43 samples). The best-fitting lines to these data suggest values of 0.071 and 0.039 kyr^{-1} for the decay constants of these species, although the latter value especially is subject to some uncertainty. The data do not support a further subdivision to separate L and LL chondrites. Repeating the same method described above to derive a relationship between weathering over time and loss by erosion, a plot of $\ln(R_{av})$ versus $\ln t$ for the separate chondrite groups yields values of $a=0.219$ and $b=0.236$ for H chondrites (Fig. 7a), and $a=0.0877$ and $b=0.48$ for L(LL) chondrites (Fig. 7b). Our attempts to fit the overall shape of the oxidation–frequency histograms, with 5 per cent bins for H and L(LL) chondrites separated (Figs 8a and b respectively), by equation (8) (using values of b derived from Fig. 7) give for N^* and R^* the values 10.63 and 0.39 for H chondrites, and 4.624 and 0.30 for L(LL) chondrites.

Combining the values for a, b and R^* in equation (6) yields estimates for λ of 0.066 kyr^{-1} for H chondrites, and 0.040 kyr^{-1} for L(LL) chondrites. Once again, these values are very close to those derived from the terrestrial age data alone, and also suggest that a significant source of scatter in the $R(t)$ plot of Fig. 2, and the same data binned in Fig. 5, is as a result of variations in bulk chemistry arising from different ordinary chondrite groups. Varying bin widths in the histograms has no great effect on these calculated values: for instance, using 4 per cent bins for both chondrite groups, and once again constraining equation (8) with values of b derived from Fig. 7, yields identical values for R^*.

This analysis, based on data from hot desert sites worldwide, supports our approach on a broad scale, and suggests

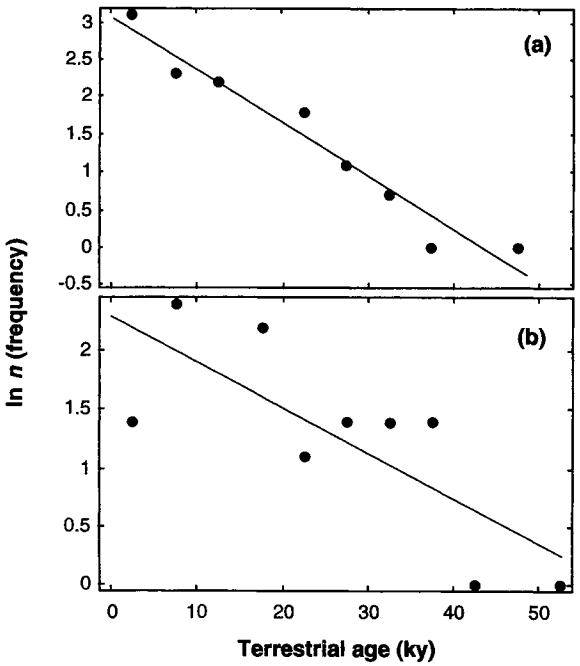

Figure 6. Ln of the number versus age in kyr for separated H (a) and L(LL) (b) chondrites. The least-squares fits to these data give $-\lambda$. We find $\lambda=0.071$ kyr^{-1} for H chondrites and $\lambda=0.039$ kyr^{-1} for L(LL) chondrites.

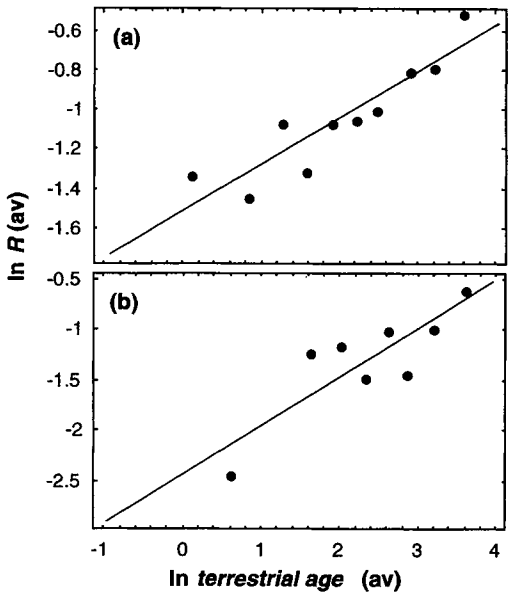

Figure 7. Ln R versus ln t for separated H (a) and L(LL) (b) chondrites.

that different ordinary chondrite groups weather at different rates. In the next section we apply the same methodology to explore the possibility that, just as differences in weathering are observed between meteorite types, so different rates of oxidation may be observed between different areas.

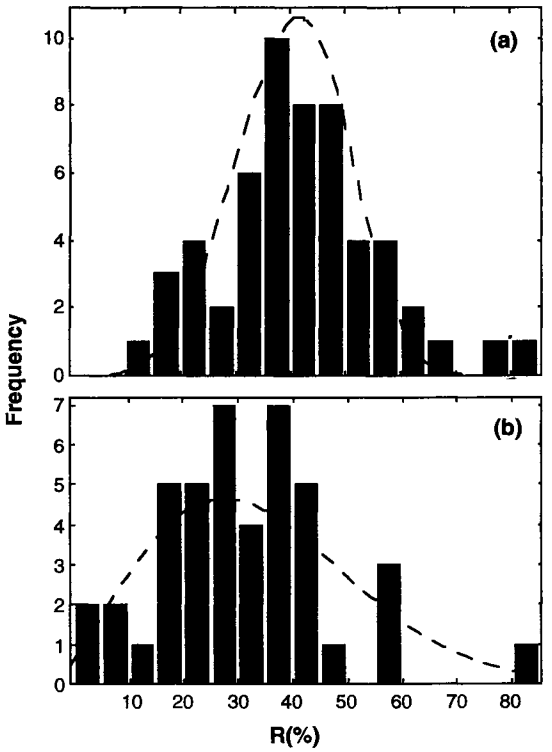

Figure 8. The data of Fig. 4 broken down to show number versus oxidation (per cent), with bins of width 5 per cent, for H (a) and L(LL) (b) chondrites. Also shown is the model fit to these data.

4.3 Individual hot desert sites

Analyses both of samples from RC and of those more recently available from the NR and the SD may be used to provide a comparison of decay constants and flux for each meteorite accumulation site separately. In Section 4.1 we considered all the hot desert sites together, with the implicit assumption that (on average) weathering has proceeded at the same rate at all three sites. However, owing to differences in climate and geomorphology between RC (Haynes 1973), the NR (Jennings 1967) and the SD (Pachur 1980), this is unlikely to be strictly true.

To explore this possibility of regional variation, we split our data into two groups. One set consists of all 63 SD samples and the other consists of the remaining 35 samples from RC and the NR, where for this study we did not distinguish between H and L(LL) ordinary chondrites. The histograms of number versus oxidation for these two groups are clearly different, with the combined RC–NR meteorites (Fig. 9a) peaking at a significantly higher R^* than the SD meteorites (Fig. 9b). We would suggest that R^* is a property of the physical weathering of ordinary chondrite meteorites, and in principle should be the same for all collection areas. A difference in R^* between sites would therefore relate to some process preferentially removing either young unweathered meteorites or old weathered meteorites. In the case of the SD, we suggest that the observed difference in R^* may be a result of the relative maturity of the different collection surfaces. Independent evidence indicates that the meteorite accumulation surface in the Sahara may have been stable only for the last 15 000–20 000 yr: the Libyan

desert to the east was undergoing continued erosion up until 14 000 yr ago (Pachur 1980). Our data tend to support this, indicating that meteorites from the SD have experienced reasonably low levels of weathering. In addition, whilst meteorites from RC and NR comprise only a third of our data set, they contain twice as many samples with terrestrial ages over 20 000 yr. Both of these lines of evidence suggest that the SD meteorites represent a relatively immature population, for which weathering may not have seriously begun to remove meteorites, and indicate that a more realistic value for R^* may be the (higher) value derived from the combined RC–NR population. Worth noting here is the observation that relatively few meteorites with recent terrestrial ages are found in the RC population (Jull et al. 1991). Whether this is a statistical anomaly, given a small data set, or a real feature of this accumulation site remains unclear.

As discussed earlier, previous attempts to calculate a decay constant for a meteorite population have suffered from limited terrestrial age data. Our analysis provides an alternate method. Applying this method to all age-dated RC samples (17 in number) gives the fit to $R(t)$ shown in Fig. 10(a), where $a=0.154$ and $b=0.383$ [in this case the small number of data points does not support separation of the meteorites into H and L(LL) chondrite groups]. To estimate the decay constant by this method we need, besides the values for a and b, a value for R^*. As the number of terrestrial age-dated RC samples totals only 17, we choose to estimate R^* from the histogram for RC and NR together (see Fig. 9a). For this figure $R^*=0.46$ and our rough estimate for the decay constant by this method is $\lambda=0.032\ \mathrm{kyr}^{-1}$ for RC, using equation (6). We note that the major source of error in our estimate of λ for the RC population is our value for R^*: more data would enable a better fit of equation (8) to a histogram of N versus R and a more accurate value for R^*.

Using the same methodology as described above for the RC population, it is also possible to establish a decay constant for the NR meteorites (18 samples). We find that the fit to $R(t)$ in Fig. 10(b) gives $a=0.273$ and $b=0.146$. Using again $R^*=0.46$ gives an estimate for λ of $0.024\ \mathrm{kyr}^{-1}$.

Although the data set is relatively small, it is possible to check our estimates of λ derived above for RC and the NR against an average decay constant derived from terrestrial age frequencies for both of these sites combined. The result, shown in Fig. 11, is a value for λ of $0.047\ \mathrm{kyr}^{-1}$, higher than our previous estimates but still within any probable errors for this analysis.

Using the fit to $R(t)$ in Fig. 10(c) for SD samples yields $a=0.174$ and $b=0.228$. Taking this value of b to constrain

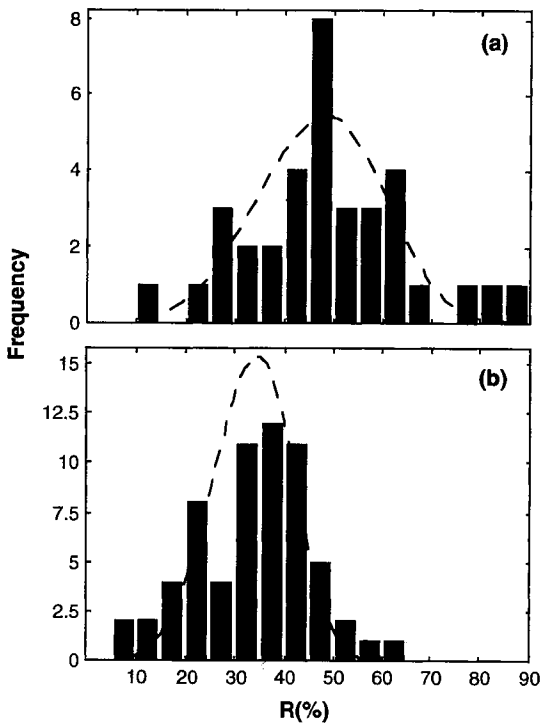

Figure 9. Oxidation–frequency histogram comparing the RC and the NR (a): hot desert accumulation sites to the SD (b). Bin widths are 5 per cent. A comparison with the model (equation 8) is also shown.

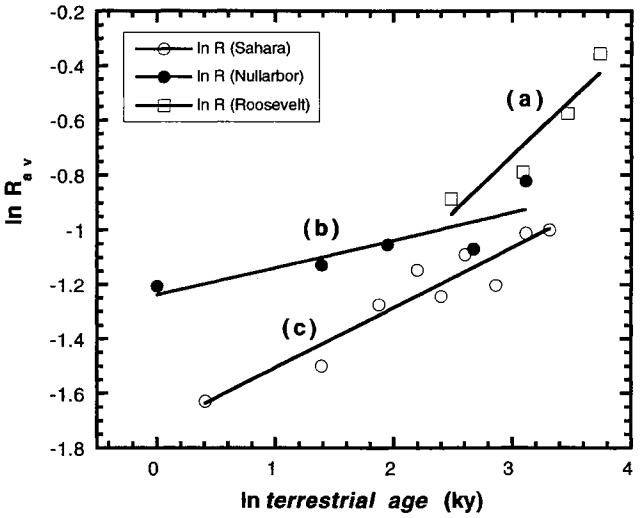

Figure 10. Ln R versus ln t (kyr) for each of the three hot desert areas, RC (a), NR (b) and SD (c).

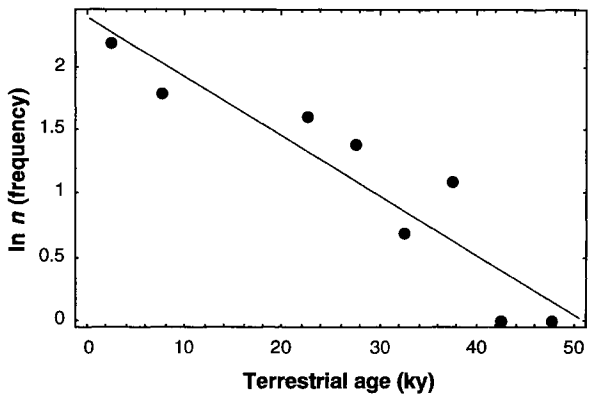

Figure 11. Ln of the number versus age in kyr for RC and NR data. The least-squares fit to these data gives $\lambda=0.047\ \mathrm{kyr}^{-1}$.

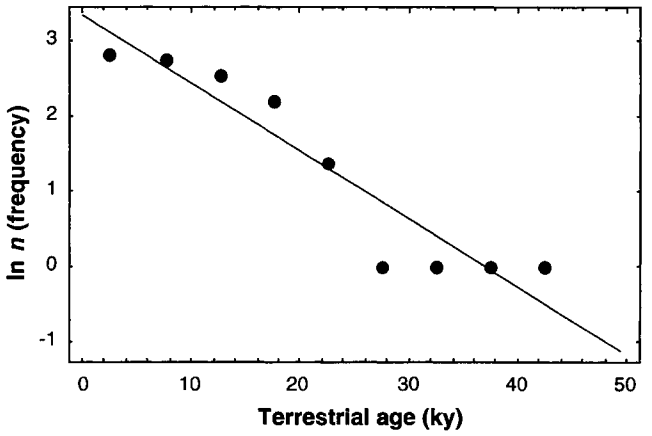

Figure 12. Ln of the number versus age in kyr for SD data. The least-squares fit to these data gives an estimate of $\lambda = 0.09$ kyr^{-1}.

equation (8), we find $N^* = 15.4$ and $R^* = 0.32$ when applied to the Saharan oxidation–frequency distribution (Fig. 9b). Clearly, there is not such good agreement between model and data in this case as in previous examples, and this may relate to factors discussed previously that are specific to SD meteorites, i.e., the immaturity of this population resulting in a relatively large number of young, lightly weathered samples. Taking these data at face value yields an estimate of λ of 0.05 kyr^{-1}; however, if we use the higher value for R^* derived from the RC–NR, as may be reasonable given our earlier discussion, we arrive at a significantly lower value for λ of 0.011 kyr^{-1}. A direct plot of $\ln(n)$ versus age (Fig. 12) yields a least-squares value for λ of 0.09 kyr^{-1}, and is subject to some error. In this case, it is likely that the lower values of λ are a better estimate of the decay constant for this area: although part of our model is based on an oxidation–frequency distribution, which is sensitive to a deficit of highly weathered samples, this is constrained by values derived from $R(t)$ which will be more robust in the face of a lack of data in some portion of the oxidation–age distribution. A simple terrestrial age–frequency distribution will be more sensitive to, say, a deficit in older samples, which would tend to give an artificially high value for λ.

Taking into account potential problems with the Saharan population, to derive an estimate of flux for each area we not only require an estimate of the decay constant, but also information relating to the meteorite population density and mass distribution on the ground (as indicated by equation 2). In the next section we discuss the acquisition of these data.

5 DENSITY AND MASS DISTRIBUTION

Sound population statistics, combined with geomorphological knowledge of the area, terrestrial ages of the meteorites and the ages of the surfaces on which the meteorites are found, are vital to an accurate determination of the flux of meteorites to the Earth. The pitfalls of including errors in only one of these parameters in calculations have been demonstrated by Zolensky et al. (1990, 1992) for meteorites from RC. Aside from estimating decay constants for meteorite accumulation sites, the derivation of meaningful population data for an area (essentially the mass distribution and population density of individual meteorites on the ground today) is a non-trivial study in its own right. The most significant problem here lies in assessing the degree to which a population has been adequately paired. Meteorites are commonly paired on the basis of chemical and textural similarities between samples, and the geographical proximity of fragments; however, it is possible to apply some independent criteria to check the completeness of a pairing study. Both the mass distribution and the terrestrial ages of meteorites from a particular area can provide a check on the effectiveness of a pairing study (Huss 1990, 1991; Jull et al. 1995), in the first case by comparing the resulting distribution to the mass distribution of modern falls, and in the second case by investigating any group of fragments that have very similar terrestrial ages. However, it must be borne in mind that data based on pairing studies represent a lower limit on the population density and mass distribution of samples in an area: all meteorites, and all fragments of a paired fall, are unlikely to be recovered.

In this section we discuss population data for the RC, NR and SD accumulation sites. When population density and mass distribution data are combined with our decay constants (in equation 2), we are able to derive three independent estimates of flux. Whilst density will vary from site to site (due to the decay rate of meteorites and the maturity of the accumulation surface), the overall mass distribution should be the same. In this initial analysis, however, we draw upon mass distributions for each area individually, as this offers a test of the overall accuracy of this data, and also follows the principle that individual estimates of flux from a given site should be self-consistent.

5.1 Roosevelt county

The great majority of RC meteorites were recovered from wind blowout areas where soil has been removed down to the hardpan (Huss & Wilson 1973). 10.8 km^2 of the larger blowouts were searched, from which all the terrestrial age-dated samples were recovered. An additional small deflation surface of 0.2 km^2 which has an anomalously recent age of 16 000 yr (Zolensky et al. 1990) has not been included in this study: only three samples were recovered from this area, none of which was terrestrially age-dated. The larger deflation areas have surface ages of between 53 500 and 95 200 yr (Zolensky et al. 1992), which correlates well with the fact that terrestrial ages for RC meteorites extend up to, and sometimes beyond, 40 000 yr (Jull et al. 1991). Zolensky et al. (1990) conducted an extensive study of pairing within the RC population, using mainly geographic proximity between fragments and textural and chemical similarities. Taking into account pairing of different fragments of the same meteorite, a total of 39 distinct meteorite falls over 10 g in mass were recovered from these larger blowout areas (Zolensky et al. 1990).

The earlier work of Zolensky et al. (1990) reported a pairing study of the RC population, which, as well as establishing the number per unit area of individual meteorite falls on the ground, also gave their mass distribution: if N is the number of mass equal to or greater than M g, then $N = \text{constant} \times M^{-0.54}$, so that a plot of $\log N$ versus $\log M$

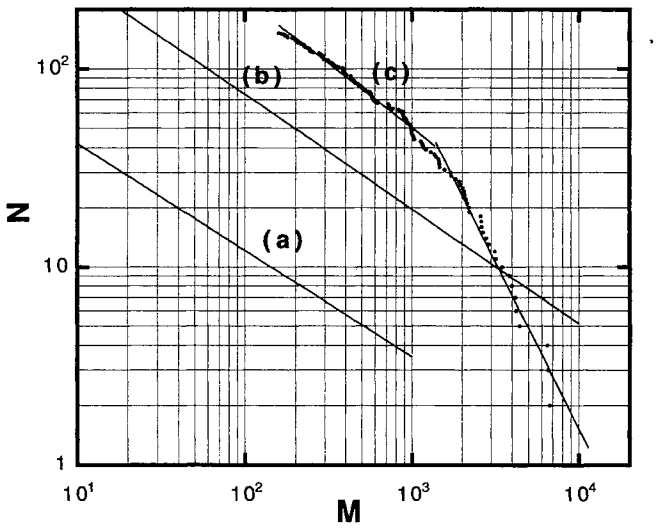

Figure 13. Mass distribution of paired meteorites recovered from all three hot desert regions, RC (a), NR (b) and SD (c), where N is the number of meteorites recovered with mass greater than M g.

has slope -0.54 (Fig. 13a). We use this mass distribution for RC meteorites.

5.2 Nullarbor Region

To date, samples from some 447 probably distinct meteorites have been described from the entire Australian continent (Bevan 1996). More than 50 per cent of these recoveries have been found in the NR, a limestone desert area of 240 000 km^2 straddling the border between Western and South Australia. In addition, several thousand fragments of an as yet unknown total number of meteorites have been recovered in recent years by careful ground-searching, the great majority of which are ordinary chondrites.

For most of the stony meteorites collected from the NR, careful consideration has been given to pairing (cf. Bevan & Binns 1989a,b; Bevan & Pring 1993); several shower falls have also been collected and their strewnfields, which remained relatively undisturbed, have been mapped (e.g. Cleverly 1972). Population statistics also indicate that there are few undetected pairs amongst meteorites so far described from the Western Australian Nullarbor (Bevan 1992a; Koeberl, Delisle & Bevan 1992), and terrestrial age data (Jull et al. 1995) indicated no evidence of selection of meteorites of a particular terrestrial age.

Unlike RC meteorites, NR samples appear to be lying on, or near, the surfaces on which they fall (Bevan 1992a, b). In the NR, within the limits of the data set currently available, the distribution of ^{14}C terrestrial ages of chondritic meteorites show an uninterrupted exponential decrease from the present day to about 30 kyr BP. The oldest terrestrial age of a stony meteorite yet dated from the NR (33.4 ± 2.3 kyr) is in good agreement with the estimated age (~ 30 kyr) of the present calcareous clay cover of the southern part of the Nullarbor Plain (*sensu stricto*) (Benbow & Hayball 1992). Perhaps the most stable hot desert meteorite accumulation surface in existence, in the context of this present study the NR provides a valuable baseline for comparison with other accumulation sites.

A large, well-documented sample of randomly searched areas of the NR totalling 44.9 km^2 yielded 45 apparently distinct meteorite finds. Thus we have a minimum density (n_{tot}/A) of approximately 1 meteorite km^{-2}. Intensive collecting within the strewnfield of the Camel Donga eucrite shower (cf. Cleverly, Jarosewich & Mason 1986), which covers an area of approximately 6.5 km^2, has so far yielded at least 16 meteorite specimens representing nine distinct meteorite falls. Together with the Camel Donga eucrite, this suggests a density of 1.5 meteorite km^{-2}. If we take the population of 317 documented and classified fragments recovered by systematic searches, then when pairing is considered, we arrive at a population of 226 distinct meteorites over 10 g in mass. The mass distribution of these samples [number of falls (N) over mass M g] yields a slope of -0.58 (Fig. 13b).

5.3 Sahara Desert

In the SD, meteorites have been recovered mainly from stony (Hammadah) desert regions, often flat, pale-coloured caliche. Large numbers of fragments (in excess of 500) have been recovered from areas of the Algerian and Libyan Sahara, mainly by searching from four-wheel-drive vehicles. Only larger stones are found by this method: 90 per cent are over 150 g; however, it is likely that most large meteorites within the search area will be identified. Given the distance travelled (and approximate field of view of the searcher), we can therefore estimate a density of larger meteorites on the ground.

A pairing study of the SD meteorites was conducted by Bischoff & Geiger (1995). These workers used parameters of find location, degree of shock metamorphism, weathering, and mineral chemistry to pair 465 fragments from the SD. Taking pairing into consideration, and field data provided by the finder, yields an approximate estimate of 1.4 meteorites over 150 g per km^2 on the ground (Bischoff, personal communication).

After pairing, it appears that 152 meteorites of mass greater than 140 g have been recovered from the region of Reg el Acfer in the Algerian Sahara (Bischoff & Geiger 1995), the area from which most of the terrestrial age-dated samples come. Masses of paired meteorites from this region are taken from Bischoff & Geiger. Considering the number of falls (N) over mass M g (shown in Fig. 13c), it is clear that there is a change in slope: the mass distribution for meteorites on the ground with mass less than 1.3 kg has slope -0.67, and for meteorites greater than 1.3 kg the slope is approximately -1.7.

6 DISCUSSION

6.1 Errors

Uncertainties in our final estimates of flux are likely to arise from (i) errors in the fit to the $R(t)$ curve (due to the scatter and experimental error), which give rise to an uncertainty in our values for a and b, (ii) the model fit (from equation 8) to the oxidation–frequency histogram, leading to an error in estimates of R^* and b, (iii) incomplete pairing within a population, which will lead to an overestimate in the number of falls and also a relatively steep mass distribution

slope and, finally, (iv) incomplete collection and/or a small collection area, which may lead to an underestimate of falls in the first case, and an overestimate in the second case due to the strewn-field effect (see Section 2).

To get an idea of the accuracy of our flux estimates, we consider that the worst non-systematic error would arise if the absolute values of all sources of error were added together. Taking the differential of equation (2), dividing by n_0, and taking absolute values, we find the maximum relative error in n_0 to be

$$\left|\frac{\Delta n_0}{n_0}\right| \leq \left|\frac{\Delta \lambda}{\lambda}\right| + \left|\frac{\Delta n_{\text{tot}}}{n_{\text{tot}}}\right|. \tag{10}$$

Also, the maximum relative error in λ follows similarly from equation (7):

$$\left|\frac{\Delta \lambda}{\lambda}\right| \leq \left|\frac{\Delta b}{1-b}\right| + \left|\frac{\Delta t^*}{t^*}\right|. \tag{11}$$

It appears likely that the relative error in n_{tot} is ultimately the greatest source of error. For instance, when all 98 samples are taken together (Figs 4 and 5) we estimate conservatively $|\Delta\lambda/\lambda| \leq 0.04 + 0.16$. It would be expected, however, that for our data the relative error $|\Delta n_{\text{tot}}/n_{\text{tot}}|$ could be greater than this. Improved systematic data collection will, of course, lower these errors, and also open the possibility of applying equation (9) directly to estimate the flux n_0.

These considerations lead us to derive an overall error on the estimate of flux from RC and NR of approximately a factor of 2 to 3. In the case of the SD population, other evidence (see our previous discussion) suggests that our calculated value of R^* for these meteorites may be low. By comparison, the calculated error quoted for the camera network data is a factor of 2 (Halliday et al. 1991), due to uncertainties in deriving a dynamical mass from the photographic trails of fireballs. The errors we derive are of a similar order, indicating that the results of these two approaches may be compared directly.

6.2 Mass distribution

A consideration of the mass distribution data from each of the three sites (Fig. 13) yields several important observations. First, the slope of the mass distribution in the lower mass range (< 1 kg) is similar for all sites, varying between -0.54 (RC, from Zolensky et al. 1990), -0.58 (NR, this study) and -0.67 (SD, from tabulated masses in Bischoff & Geiger 1995). These values are near, though consistently less than, the value of -0.49 calculated by Halliday et al. (1989) from the camera network study. The fact that our values are lower than that of Halliday et al. (1989) is probably due to incomplete pairing, particularly in the SD population.

Secondly, the change in slope in the mass distribution for SD samples is significant. A similar change was observed in the mass distribution derived from fireball data (Halliday et al. 1989) at approximately 1 kg, and was attributed to the greater likelihood of larger meteorites fragmenting in the atmosphere. Thus it appears that processes affecting the mass distribution of incoming meteoroids may be preserved in populations of hot desert meteorite finds. That a similar distribution is not observed for RC may be due to the relatively small number of samples recovered from this region: meteorites of large mass are not sampled. However, this does not apply in the case of the NR. Another plausible explanation relates to pairing. The parameters commonly employed to pair meteorite fragments (except perhaps geographic proximity) are unlikely to distinguish between meteoroids that fragmented in the upper or lower atmosphere. As such, it appears possible that pairing studies may act to remove the change in slope observed at 1 kg. The above discussion indicates that pairing in the SD population may not be complete; therefore for this area a signature of the incoming mass distribution remains. This observation has important implications when comparing meteorite accumulation site and direct observational estimates of flux. It also suggests that in order to resolve the flux and mass distribution for higher mass bodies it may be necessary to look again at the parameters we use to pair samples.

6.3 Flux estimates

Although our decay constants were calculated solely from ordinary chondrites, in this preliminary analysis we do not distinguish between these and other meteorite groups. The population density data represent all meteorites found in this region: as such, we do not scale our data to account for any ordinary chondrite bias. In addition, the overall effect of extrapolating ordinary chondrite decay constants to the entire population is likely to be minor, largely because ordinary chondrites account for approximately 80 per cent of observed falls.

To obtain an estimate of flux, $n_0(m)$, for each accumulation site, we relate our calculated values for λ to the density of paired meteorites over a given mass per unit area, n_{tot}/A, in equation (2). For example, in the case of the RC meteorites, λ is 0.032 kyr, and the density of meteorites km^{-2} on the ground over 10 g in mass is 39/10.8, which is 3.611. Given these data, our flux calculation, for events over 10 g in mass per 10^6 km^{-2} yr^{-1}, is $0.032 \times 3.611 \times 1000$, which yields an estimate of 116 events. We can extrapolate this estimate to larger masses by using the slope of the mass distribution for each site. In the case of RC this is -0.54, so to extrapolate to events over 500 g from our initial 10 g we take $50^{-0.54} \times 116$, which is approximately 14. In this manner, given the decay constant, mass distribution and density data for each site, we can calculate flux for approximately the 10 g to 1 kg mass range.

Estimates of flux derived from our study, Zolensky et al. (1990) and those of Halliday et al. (1989) are presented in Table 1. What is clear from this comparison is that estimates derived from RC and the NR agree well with the earlier estimate of Halliday et al. (1989), and also with one another, differing by only a factor of 2 to 3 throughout the entire mass range. The estimate from the SD, using the lower value for R^* derived from the SD oxidation-frequency curve (Fig. 9b) is relatively high (approximately a factor of 3 to 4 above the others); however, if the lower estimate of λ (using R^* calculated from the RC–NR population) is used, then we obtain an estimate of flux very close to that derived from the other sites. The agreement between our estimates, and also with the camera network data, is remarkable, particularly given the very different methodologies employed. The

Table 1. Predictions of N_0, the frequency of events per 10^6 km^2 yr^{-1} larger than the total mass M_T, comparing data from accumulation sites and camera observations of present-day flux (after Halliday et al. 1989). Also shown are values of λ for individual sites, and the combined mass flux, $\sum M$(kg), over the 10–10^3 g mass range accreted to the Earth per year.

	λ (ky^{-1})	m_T 1 kg	500 g	150 g	100 g	50 g	20 g	10 g	$\sum$M(kg)
Zolensky et al. 1990		78.2	114	218	271	394	647	940	
Halliday et al. 1989		8.7	12	22	27	38	59	83	3900
Roosevelt	0.032	9.6	14	27	33	48	79	116	7300
Nullarbor	0.024	2.5	3.7	7.5	9.5	14	24	36	2900
Sahara (R^* = 0.46)	0.011	4.3	6.9	15	20	32	60	95	14100
Sahara (R^* = 0.32)	0.050	19.7	31	70	92	147	271	431	64400

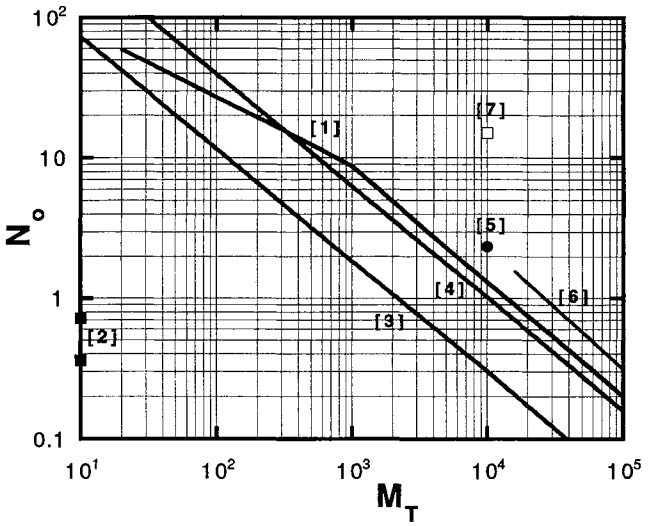

Figure 14. Previous observational estimates of the present flux of meteorites: camera network data [1] (Halliday et al. 1989) with estimates based on recovery of observed falls worldwide [2] (Buchwald 1975), [3] (Brown 1960), [4] (Brown 1961), [5] (Hawkins 1960), [6] (Hughes 1980) and [7] (Millard 1963), where N_0 is the number of events per 10^6 km^2 yr^{-1} for mass larger than M_T g. Brown (1960, 1961) quotes maximum and minimum values of flux; the data presented here are an average.

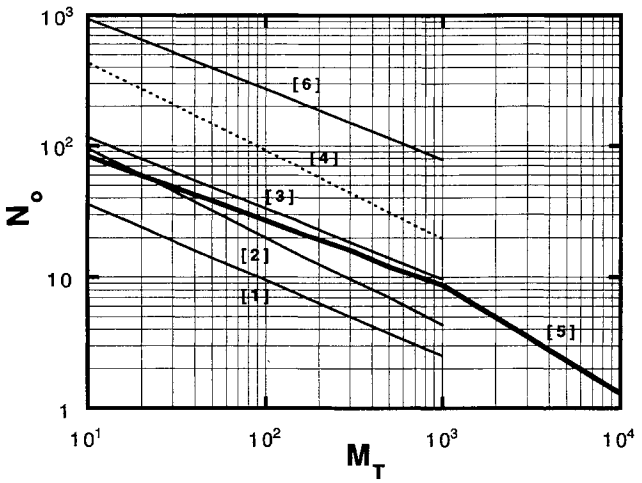

Figure 15 Our estimates of flux ([1] (NR), [2] (SD with $R^* = 0.46$), [3] (RC), [4] (SD with $R^* - 0.32$)) compared to the best observational estimates of the present flux of meteorites [5] (Halliday et al. 1989) and a previous estimate from the RC accumulation site [6] (Zolensky et al. 1990), N_0 is the number of events per 10^6 km^2 yr^{-1} for mass larger than M_T g.

results suggest that the integrated flux of meteorites to the Earth over the last 50 000 yr has remained essentially unchanged, a finding that is in agreement with current models of the orbital evolution of asteroids.

It is also possible to derive the total mass flux for the meteorite size range, enabling a direct comparison with the cosmic dust and micrometeorite fraction. Our study constrains the mass distribution over the relatively restricted range from 10 g to 1 kg. Integration over this mass range (see Appendix A for the method) yields an average mass flux from our data of 8100 ± 4600 kg (see Table 1) for the Earth per year, not including the low-R^* SD value. If the SD mass distribution slope is low due to incomplete pairing (as seems likely, given our previous discussion), and a more realistic value for the 10 g to 1 kg size range lies in the region of -0.5 to -0.6, then the total mass flux may be constrained to between 2900 and 7300 kg yr^{-1}, i.e., the values for the NR and RC populations. Using the Halliday data for >1 kg masses to derive the total mass flux to the Earth in the meteorite size range (10–10^6 g) yields a value of 5.38×10^4 kg yr^{-1}. It is noteworthy that the bulk of the mass is concentrated in the larger meteoroids, and also that this value is a small fraction of the total cosmic dust/micrometeorite mass flux (see Section 1).

Previous estimates of the meteorite flux, based on observed falls and direct observation using camera networks, are presented in Fig. 14. A comparison between estimates arising from this present study, the best observational estimate (taken to be Halliday et al. 1989), and previous data from accumulation sites, is shown in Fig. 15. What emerges from this review is that, in the past, observational data have yielded a wide range of estimates for the present-day flux of meteorites to the Earth. We consider the data of Halliday et al. (1989) to be the best estimate of present flux, derived from data resulting from the 11-yr

operation of the MORP camera network. Although Brown (1961) and Hughes (1980) derive estimates that fall close to the value of Halliday et al. (1989), it is clear that the assumptions involved in calculating flux from eye-witnessed falls can give rise to large errors: estimates by Hawkins (1960), Brown (1961), Millard (1963) and Buchwald (1975) differed by several orders of magnitude.

Analyses based on data from meteorite accumulation sites have shown a similar variation. Previous attempts have differed by approximately a factor of 7 (Huss 1990), and by more than an order of magnitude (Zolensky et al. 1990) from the estimate of Halliday et al. (1989), although these authors acknowledge (Zolensky et al. 1992) that this is most likely to be a result of poorly constrained models based on limited data. This is unfortunate, as although current models of the delivery of meteorites to the Earth do not predict a change in flux over the 50 000-yr period sampled by hot desert meteorite accumulation sites, it is possible that over the 10^6-yr time-scale represented by the Antarctic population, changes may have occurred. Analysing data from meteorite accumulations is the only method available by which a temporal variation in meteorite flux might be detected. A first step, however, is to show that a meaningful flux estimate may be calculated from 'younger' populations. Our analysis, based on a much larger data set than previous studies and employing a technique that provides a direct measure of the degree of oxidation experienced by a sample, suggests that meteorite accumulation sites may be used to provide a reliable estimate of flux.

7 CONCLUSIONS

Our work suggests that a consideration of Mössbauer spectroscopic and ^{14}C terrestrial age data provides an effective means of monitoring weathering over time between different meteorite groups and hot desert accumulations sites, and enables decay constants for meteorite populations to be calculated. It also indicates that, with a suitable methodology and adequate attention to some of the problems involved, areas of meteorite accumulation may yield an estimate of flux that is consistent between sites and reasonable in the context of current models of the orbital evolution of asteroids and present-day estimates of flux. The most important result that emerges from this work is that, contrary to earlier estimates from accumulation sites, the time-integrated flux of meteorites to the Earth over the last 50 000 yr is the same as that observed at the present day. A number of other conclusions may also be drawn.

(1) Weathering over time for hot desert meteorite populations may be modelled using an appropriate power law. In addition, oxidation frequency data (for the RC–NR population) indicate a turnover at approximately 45 per cent oxidation (as measured by Mössbauer spectroscopy). This relates to the physical weathering of ordinary chondrites: pore spaces are filled by oxides and clay minerals, at which point further oxidation acts to fragment the sample.

(2) The mass distribution of samples recovered from hot desert accumulation sites shows a similar morphology to that derived from photographic observations of fireballs, with a change in slope in the region of 1 kg. This indicates that a change due to some mass dependence, relating to ablation and fragmentation in the atmosphere, is preserved in samples on the ground.

(3) Differences in weathering rate are observed between H and L(LL) chondrites, and also between the different hot desert accumulation sites. In the first case this is due to bulk chemistry, and in the second to variation in climate and geomorphology between sites. The fact that, even at the current level of resolution, our analysis is sensitive to these factors indicates that a larger data set may allow a significant refinement in a calculation of flux.

(4) The total mass flux to the Earth in the 10 g to 1 kg size range is constrained to between 2900 and 7300 kg yr^{-1} (the MORP study yields an estimate of 3900 kg yr^{-1}).

Whilst deriving a more accurate estimate of the flux of meteorites using an observational method (such as MORP; Halliday et al. 1989) would require a large investment, estimates based on accumulation site data are straightforward and inexpensive. In the future, more detailed pairing studies and larger collections of meteorites, both of which already form the basis of ongoing curatorial work, will yield more accurate estimates of the population density of meteorite samples on the ground and their mass distribution. Together with a larger terrestrial age and oxidation data set, and the methodology outlined above, this should lead to increasingly better constrained estimates of the flux of meteorites to the Earth.

ACKNOWLEDGMENTS

We thank Addi Bischoff for providing recovery data relating to the Saharan population, and Mike Ayres for proofreading. Meteorite samples were obtained from the Western Australian Museum, Perth, the Natural History Museum, London, and the Max Planck Institut für Chemie, Mainz. We also thank the staff of the NSF Arizona AMS facility for ^{14}C measurements. The Arizona work was supported by NASA grant NAGW-3614 and NSF grant EAR 92-03883. PAB acknowledges support from the EC under contract number SCI*-CT91-0618(SSMA) while part of this work was carried out.

REFERENCES

Barker J. L., Anders E., 1968, GCA, 32, 627
Barlow N. G., 1990, Geol. Soc. Am., Spec. Paper, 247, 181
Benbow M. C., Hayball A. J., 1992, Australian Caver, 130, 3
Benoit P. H., Bland P. A., Berry F. J., Pillinger C. T., 1996, Meteoritics and Planetary Science, submitted
Bevan A. W. R., 1992a, Records of the Australian Museum, Suppl., 15, 1
Bevan A. W. R., 1992b, Meteoritics, 27, 202
Bevan A. W. R., 1996, J. R. Soc. West. Austr., in press
Bevan A. W. R., Binns R. A., 1989a, Meteoritics, 24, 127
Bevan A. W. R., Binns R. A., 1989b, Meteoritics, 24, 135
Bevan A. W. R., Pring A., 1993, Meteoritics, 28, 600
Bibron R., Chesselet R., Crozaz G., Leger G., Mennessier J. P., Picciotto E., 1974, WPSL, 21, 109
Bischoff A., Geiger T., 1995, Meteoritics, 30, 113
Bland P. A., Berry F. J., Pillinger C. T., 1995, in Schultz L., Annexstad J. O., Zolensky M. E., eds, Workshop on Meteorites from

Cold and Hot Deserts. LPI Technical Report 95-02, Houston, p. 22
Bland P. A., Berry F. J., Smith T. B., Skinner S. J., Pillinger C. T., 1996a, GCA, 60, 2053
Bland P. A., Kelley S. P., Berry F. J., Cadogan J. M., Pillinger C. T., 1996b, American Mineralogist, submitted
Brown H., 1960, J. Geophys. Res., 65, 1679
Brown H., 1961, J. Geophys. Res., 66, 1316
Buchwald V. F., 1975, Handbook of Iron Meteorites, Vol. 1. Iron Meteorites in General. Univ. California Press, Berkeley, p. 38
Cleverly W. H., 1972, J. R. Soc. West. Austr., 55, 115
Cleverly W. H., Harosewich E., Mason B., 1986, Meteoritics, 21, 263
Esser B. K., Turekian K. K., 1988, Geochim. Cosmochim. Acta, 52, 1383
Farley K. A., 1995, Nat, 376, 153
Farley K. A., Patterson D. B., 1995, Nat, 378, 600
Ganapathy R., 1983, Science, 220, 1158
Grieve R. A. F., 1984, J. Geophys. Res., 89, B403
Grün E., Zook H. A., Fechtig H., Giese R. H., 1985, Icarus, 62, 244
Halliday I., Blackwell A. T., Griffin A. A., 1989, Meteoritics, 24, 173
Halliday I., Blackwell A. T., Griffin A. A., 1991, Meteoritics, 26, 243
Hawkins G. S., 1960, AJ, 65, 318
Haynes C. V., 1973, in Wendorf F., Hester J. J., eds, Late Pleistocene Environments of the Southern High Plains. Fort Burgwin Research Center, Taos, p. 57
Hughes D. W., 1980, in Halliday I., McIntoch B. A., eds, Solid Particles in the Solar System. Reidel, Dordrecht, p. 207
Huss G. I., Wilson I. E., 1973, Meteoritics, 8, 3, 287
Huss G. R., 1990, Meteoritics, 25, 41
Huss G. R., 1991, Geochim. Cosmochim. Acta, 55, 105
Imamura M., Inoue T., Nishiizumi K., Tanaka S., 1979, 6th Intl. Cosmic Ray Conf., OG 12
Jennings J. N., 1967, in Dunkley J. R., Wigley T. M. L., eds, Caves of the Nullarbor. Speleological Research Council, Univ. Sydney, Sydney, p. 13
Jull A. J. T., Wlotzka F., Palme H., Donahue D. J., 1990, Geochim. Cosmochim. Acta, 54, 2895
Jull A. J. T., Wlotzka F., Palme H., Donahue D. J., 1991, Lunar Planet. Sci. Conf., 24, 667
Jull A. J. T., Donahue D. J., Cielaszyk E., Wlotzka F., 1993a, Meteoritics, 28, 188
Jull A. J. T., Wlotzka F., Bevan A. W. R., Brown S. T., Donahue D. J., 1993b, Meteoritics, 28, 376
Jull A. J. T., Bevan A. W. R., Cielaszyk E., Donahue D. J., 1995, in Schultz L., Annexstad J. O., Zolensky M. E., eds, Workshop on Meteorites from Cold and Hot Deserts. LPI Technical Report 95-02, Houston, p. 37
Koeberl C., Delisle G., Bevan A. W. R., 1992, Die Goewissenschaften, 8, 220
Kyte F. T., Wasson J. T., 1986, Science, 232, 1225
Love S. G., Brownlee D. E., 1993, Science, 262, 550
Maurette M., Jehanno C., Robin E., Hammer C., 1987, Nat, 328, 699
Millard H. T. Jr, 1963, J. Geophys. Res., 68, 4297
Murrell M. T., Davis P. A. Jr, Nishiizumi K., Geochim. Cosmochim. Acta, 44, 2067
Ozima M., Takayanagi M., Zashu S., Amari S., 1984, Nat, 311, 448
Pachur H.-J., 1980, in Salem M. J., Busrewil M. T., eds, The Geology of Libya. Academic Press, London, p. 781
Robinowitz D. L., 1993, ApJ, 407, 412
Shoemaker E. M., Wolfe R. F., Shoemaker C. S., 1990, Geol. Soc. Am. Spec. Paper, 247, 155
Takayanagi M., Ozima M., 1987, J. Geophys. Res., 92, 12531
Taylor A. D., 1995, Icarus, 116, 154
Zolensky M. E., Wells G. L., Rendell H. M., 1990, Meteoritics, 25, 11
Zolensky M. E., Rendell H. M., Wilson I., Wells G. L., 1992, Meteoritics, 27, 460

APPENDIX A

Deriving the total amount of material accreted to the Earth in the meteorite size range requires integration over the mass range of interest. Halliday et al. (1989) (equations 6 and 7) give

$$\log N = \begin{cases} 2.41 - (0.49)\ \log\ m_T & \text{for } m_T \leq 1030 \text{ g} \\ 3.40 - (0.82)\ \log\ m_T & \text{for } m_T \geq 1030 \text{ g;} \end{cases}$$

$$\text{so } N(m_T) = \begin{cases} 10^{2.41} m_T^{-0.49} & \text{for } m_T \leq 1030 \text{ g} \\ 10^{3.40} m_T^{-0.82} & \text{for } m_T \geq 1030 \text{ g,} \end{cases}$$

where N is the number of mass $\geq m_T$ g per 10^6 km^2 yr^{-1}. Our analysis derives a similar relationship for each accumulation site, for masses < 1 kg:

$\log N = 2.13 - (0.58)\ \log m_T$ for the NR,

$\log N = 2.60 - (0.54)\ \log m_T$ for the RC,

$\log N = 2.65 - (0.67)\ \log m_T$ for the SD ($R^* = 0.46$),

$\log N = 3.31 - (0.67)\ \log m_T$ for the SD ($R^* = 0.32$).

If $N(m)$ is equal to the *number* per 10^6 km^2 yr^{-1} of mass greater than m, then the number per 10^6 km^2 yr^{-1} lying between m and $m + \mathrm{d}m$ is

$$N(m) - N(m + \mathrm{d}m) = -\frac{\mathrm{d}N(m)}{\mathrm{d}m}\,\mathrm{d}m.$$

So the *mass* on the ground (per 10^6 km^2 yr^{-1}) between m and $m + \mathrm{d}m$ is

$$-m\,\frac{\mathrm{d}N(m)}{\mathrm{d}m}\,\mathrm{d}m.$$

From Halliday et al. (1989) we can write

$$N(m) = \begin{cases} c_1 m^{A_1} \text{ for } m \leq 1030 \text{ g,} \\ \qquad \text{where } c_1 = 10^{2.41} \text{ and } A_1 = -0.49 \\ c_2 m^{A_2} \text{ for } m \geq 1030 \text{ g,} \\ \qquad \text{where } c_2 = 10^{3.40} \text{ and } A_2 = -0.82. \end{cases}$$

This gives

$$-m\,\frac{\mathrm{d}N}{\mathrm{d}m} = \begin{cases} -A_1 c_1 m^{A_1} & \text{for } m \leq 1030 \text{ g} \\ -A_2 c_2 m^{A_2} & \text{for } m \geq 1030 \text{ g.} \end{cases}$$

Considering all masses between m_L and m_U (where $m_L \leq 1030$ g and $m_U \geq 1030$ g), the total mass per 10^6 km^2 yr^{-1} is

$$M = \int_{m_L}^{1030} -A_1 c_1 m^{A_1}\,\mathrm{d}m + \int_{1030}^{m_U} -A_2 c_2 m^{A_2}\,\mathrm{d}m$$

$$= -\left(\frac{A_1 c_1}{A_1+1}\right)[(1030)^{A_1+1} - (m_L)^{A_1+1}]$$

$$-\left(\frac{A_2 c_2}{A_2+1}\right)[(m_U)^{A_2+1} - (1030)^{A_2+1}].$$

Taking the above values for A_1, c_1, A_2 and c_2 from Halliday et al. (1989), between $m_L = 10$ g and $m_U = 10^6$ g, we find $M = 105.3$ kg per 10^6 km^2 yr^{-1}. Given that the surface area of the Earth is 5.11×10^8 km^2, this analysis would suggest a total mass flux to the Earth in the meteorite size range of 5.38×10^4 kg yr^{-1}. A similar analysis is possible using data from accumulation sites (given above) in the mass range 10–10^3 g (see Table 1).